# Specific Antibody−DNA Interaction: A Novel Strategy for Tight DNA Recognition†

Santiago M. Di Pietro,‡,§,|| Juan M. Centeno,‡,§ M. Laura Cerutti,‡ M. Fernanda Lodeiro,‡ Diego U. Ferreiro,‡ Leonardo G. Alonso,‡ Frederick P. Schwarz,⊥ Fernando A. Goldbaum,‡ and Gonzalo de Prat-Gay*,‡

*Instituto Leloir and Facultad de Ciencias Exactas y Naturales, Universidad de Buenos Aires, Buenos Aires, Argentina, and Center for Advanced Research in Biotechnology, National Institute of Standards and Technology, Rockville, Maryland 20850*

*Received September 18, 2002; Revised Manuscript Received April 2, 2003*

ABSTRACT: Anti-double-stranded DNA monoclonal antibodies against a viral transcriptional regulatory site are capable of discriminating single-base replacements with affinities of $1 \times 10^{-9}$ M, which were optimized for the length of the duplex used as the immunogen. Their affinity for DNA duplexes of increasing length is lower, but reaches a plateau at $2 \times 10^{-8}$ M, still a fairly high affinity compared to those of most known natural anti-DNA antibodies. The ability of the antibodies to bind to a 166 bp DNA fragment containing the specific sequence strongly suggests that these have the potential of binding the specific sequence within larger genomic DNA fragments. Electrostatic interactions do not play a significant role, the opposite of what is observed in natural DNA binding interfaces. In addition, the insensitivity of the antibody−DNA interaction to solute effects is indicative of a marginal participation of water molecules at the interface compared to the level of participation at the natural E2−DNA interface. Spectroscopic evidence of base unstacking strongly suggests substantial denaturation of antibody-bound DNA, in agreement with thermodynamic results that show an unusual positive heat capacity change, which could be explained at least in part by the exposure of DNA bases upon binding. Lower local DNA stability cooperates with sequence recognition in producing the highest binding affinity. A slow rate of antibody−DNA association indicates an energy barrier imposed by conformational rearrangements, as opposed to an electrostatically assisted diffusion-controlled collision in the E2 DNA binding domain. While the E2−DNA interaction takes place through a typical direct readout mechanism, the anti-double-stranded DNA monoclonal antibody−DNA interaction could be viewed as a distinctive case of indirect readout with a significant distortion in the DNA conformation. However, the precise mechanism with which the DNA bases are accommodated in the antibody combining site will require structural analysis at atomic resolution. These results constitute a first stage for unveiling the unusual molecular recognition mechanism of a specific DNA sequence by antibodies. This mechanism could represent the strategy with which the immune system tightly and specifically recognizes a DNA antigen.

DNA is specifically recognized in living cells by proteins in many different ways, ranging from small domains of transcription regulatory proteins to larger enzymes related to nucleic acid synthesis and modification (*1*, *2*). Although there are numerous interface topologies and a large variability in DNA base to amino acid contacts, there are common themes through which this recognition is accomplished (*1*, *3*). In general, ionic interactions are long-range and contribute substantially to binding energy but very little to specificity, whereas hydrogen bonds are short-range and contribute less to stability but are the main determinants of specificity. Hydrophobic interactions are the result of interface desolvation that contributes to the binding energy and also to recognition through specific interactions of the nonpolar amino acids with DNA bases.

Much is known about how antibodies recognize protein antigens, where the general rules are similar to those that govern protein−protein recognition (*4*, *5*). On the other hand, there is little information about how antibodies recognize double-stranded DNA, because of the low antigenicity of DNA and the difficulties in raising antibodies against it (*6*). The most frequently found anti-DNA autoantibodies are those related to the autoimmune disease systemic lupus erithematosus (SLE) (*7*). These are not specific to particular sequences of single- or double-stranded DNA, or at least the putative specific sequences that elicit them have not been identified; it is not yet clear whether the elicitor is indeed DNA (*7*). These autoantibodies exhibit a low affinity for the generic oligonucleotides used to assay them (*8*). Recently, sequence specific recognition was proposed for an anti-

† S.M.D.P. holds a postdoctoral fellowship from Conicet (Consejo Nacional de Investigaciones Científicas y Técnicas), and M.L.C., D.U.F., and L.G.A. hold doctoral fellowships from Conicet. S.M.D.P. was partly supported by Fundación Antorchas. J.M.C. holds a Ramon Carrillo Oñativia Fellowship. G.d.P.-G. acknowledges the support of Fundación Bunge y Born and Fundación Antorchas.

* To whom correspondence should be addressed. E-mail: gpratgay@leloir.org.ar.

‡ Universidad de Buenos Aires.

§ These authors contributed equally to this work.

|| Present address: Department of Human Genetics, David Geffen School of Medicine at UCLA, Gonda Center, Room 6554, Los Angeles, CA 90095-7088.

⊥ National Institute of Standards and Technology.

10.1021/bi026866u CCC: $25.00 
Published on Web 05/03/2003

single-stranded DNA autoantibody (*9*), and a thermodynamic characterization of this system was carried out (*10*). Despite the interest that such interaction stimulates, the DNA sequences were the result of binding site selection experiments from random libraries *in vitro* (*9*), and specificity refers to the ability of the autoantibody to discriminate a sequence of single-stranded DNA (ssDNA) selected for tight binding from others, and does not refer to the sequence that elicited the antibody response.

We have obtained specific anti-double-stranded DNA monoclonal antibodies (a-DNAbs) that recognized the binding site of the E2 transcriptional regulator from "high-risk" human papillomavirus strain 16 (HPV-16) with very high affinity (*11*). This affinity matches that of the natural viral DNA binding and dimerization C-terminal domain of the E2 protein (E2C), where the antibody is able to discriminate effectively against a number of nonspecific double- and single-stranded DNA oligonucleotides with factors ranging from 125- to 20000-fold (*11*).

In the work presented here, we aim to define a recognition mechanism with which the a-DNAbs tightly interact with DNA and discriminate specific from nonspecific sequences. In particular, we wanted to focus on features that the a-DNAbs could share with the E2C domain and DNA binding proteins in general. From the factors governing the a-DNAb−DNA interaction, we clearly cannot find features in common with DNA recognition in HPV-16 E2 or other proteins that evolved for the control of gene function. On the contrary, the interaction we describe for the a-DNAbs appears to use a completely novel strategy for DNA recognition, also different from what is known about autoantibody DNA recognition. These results provide the first insight into the specific recognition mechanism of a DNA as an antigen by an elicited antibody that went through the process of affinity maturation.

## MATERIALS AND METHODS

*Proteins and DNAs*. The C-terminal DNA binding domain of the E2 protein from human papillomavirus strain 16 was expressed in BL21-DE3 *Escherichia coli* cells and purified as previously described (*35*). a-DNA IgGs were purified from the hybridoma lines described previously (*11*). Fabs were titrated weekly with DNA and were shown to retain their 100% binding activity for at least 2 months. Fab fragments of the antibodies were used for binding experiments throughout the work to simplify the binding analysis, unless stated otherwise.

The sequence of the A chain of the reference oligonucleotide is 5′-GTAACCGAAATCGGTTGA-3′, corresponding to E2 site 35 in the HPV-16 genome, where the underlined sequence indicates the consensus E2 binding site. DNA oligonucleotides were obtained from IDT. Long oligonucleotides were purified by SDS−PAGE by the manufacturer. All oligonucleotides were tested for duplex formation by native gel electrophoresis. The 166 bp DNA fragment was amplified by PCR from pUC18 where HPV-16 E2 site 35 was cloned in the multiple cloning site at *Eco*RI and *Hin*dIII sites. The product was purified using two phenol/chloroform extractions, followed by ethanol precipitation and air-drying, and finally separated from primers and nucleotides by gel filtration chromatography on Superdex 200 (Pharmacia). The purified fragment was dialyzed, lyophilized, and resuspended in volumes appropriate for the titration experiments. The concentration of the DNA duplexes was calculated from extinction coefficients (*36*).

*Fluorescence Binding Experiments*. Tryptophan fluorescence titrations were carried out with excitation at 295 nm, and the emission was monitored at 340 nm, using an Aminco Bowman Series 2 spectrofluorimeter. The proteins were incubated in TBS [25 mM Tris and 150 mM NaCl (pH 7.4)] at protein concentrations of 10−40 nM in volumes of 3.0 mL at 25 ± 0.1 °C. Double-stranded DNA oligonucleotides were gradually added, and the tryptophan fluorescence was measured after a 5 min equilibration at each point. The maximum dilution was 10%, and the fluorescence was corrected accordingly. A linear baseline was subtracted for the different tritrations, and the tight binding and large fluorescence changes that were observed did not require inner filter correction. The data were fitted using nonlinear squares to a binding model where both protein and DNA concentrations are considered (*37*).

$$[\text{Fab}-\text{DNA}] = 0.5\Delta F([\text{DNA}] + [\text{Fab}] + K_D) - [([\text{DNA}] + [\text{Fab}] + K_D)^2 - (4[\text{DNA}][\text{Fab}])]^{0.5}$$

were $\Delta F$ is the difference in the signal between the Fab−DNA complex and free Fab, [DNA] and [Fab] are the oligonucleotide and protein concentrations, respectively, and $K_D$ is the dissociation constant for the interaction. The data were corrected for dilution and for inner filter effects.

*UV Absorbance Titrations and Thermal Denaturation of DNA*. Absorbance experiments were carried out in a Jasco V-550 spectrophotometer. DNA duplexes at a concentration of 100 nM were incubated in 0.7 mL of TBS at 25 ± 0.1 °C. Concentrated ED-10 Fab was gradually added to the solution, and the absorbance at 260 nm was measured with a bandwidth of 10 nm after a 3 min equilibration period. The instrument noise was less than 0.0001 unit. The absorbance corresponding to the proteins (ED-10 and E2C) was subtracted prior to calculating delta absorbances at the saturation of binding. Thermal denaturations of DNA were carried out with similar concentrations and buffers, and the absorbance values were recorded after equilibration for 10 min at each temperature.

*Effects of Salt on DNA Binding Determined by an ELISA*. E2C contains a solvent-exposed tryptophan residue, which generates large fluorescence intensity changes responding to variations in ionic strength, introducing artifacts into the fluorescence quenching experiments. To rule out similar complications for the antibodies, we designed an ELISA experiment. Briefly, ELISA plates were coated with streptavidin (1 mg/well in TBS) for 60 min. Solutions containing 5′-biotinylated site 35 DNA with either E2C protein, ED-10, or ED-84 IgGs at a 5-fold molar excess were incubated with 1% BSA in TBS at the indicated salt concentrations. The 200 $\mu$L mix was incubated in microcentrifuge tubes for 30 min at room temperature. The entire mix was transferred to the streptavidin-coated ELISA plates for 15 min, and subsequently washed three times with TBS. The retention of E2C in the solid phase, representing the degree of binding to the biotinylated specific DNA, was developed using ED5 IgG, an anti-E2C antibody, with peroxidase-conjugated polyclonal antibodies. The DNA-bound a-DNAbs (ED-10

or ED-84) were developed directly with anti-mouse IgG peroxidase-conjugated polyclonal antibodies. For each separate tube, the same mixture was incubated in the absence of a biotinylated oligonucleotide as a blank. The resulting OD value was subtracted, normalized, and plotted as the amount of bound DNA versus NaCl concentration.

*Isothermal Titration Calorimetry (ITC).* ITC were carried out as described previously (*38*) using a Microcal Omega titration calorimeter. The dissociation binding constants in the temperature range of 293−305 K were too high to be determined from the ITC results at the high concentrations of protein that were required to detect the heats of binding. In this temperature range, only three to four titrant additions were performed and the binding enthalpy was calculated from the ratio of the area under the titration peak to the amount of DNA titrated into the sample. At the protein and DNA concentrations employed and at the high binding affinities, it can be shown that with each addition of titrant below saturation the amount of DNA bound to the protein is >99%. At the high-temperature limit, the binding affinity is weaker so that a binding constant can be determined from a fit of a 1:1 binding model to the binding isotherm. All heats of binding were corrected for the endothermic heat of dilution of the DNA as determined in a titration of the DNA into buffer. Calculation of entropies in Table 2 was based on equilibrium dissociation constants measured from the fluorescence quenching experiments.

*Circular Dichroism.* Near-UV circular dichroism spectra of free and bound DNA were recorded in a Jasco J-810 spectropolarimeter. Ten scans were averaged, and the raw ellipticity is shown, since the DNA concentration was identical in all the samples. Experiments were carried out at 25 ± 0.1 °C, and buffer baselines were subtracted from all spectra.

## RESULTS

*DNA Length and Sequence Determinants of Binding Affinity.* Monovalent Fab fragments of two monoclonal a-DNAbs, ED-10 and ED-84, are capable of high-affinity stoichiometric binding and sequence discrimination against nonspecific duplexes and single-stranded DNA with changes in binding free energies ranging from 3.1 to 5.8 kcal/mol (*11*). We first directed our attention to defining sequence and length determinants of the DNA ligand, focusing on the ED-10 a-DNAb as an example, with site 35-18, the oligonucleotide used to obtain the a-DNAbs (*11*), as the reference DNA duplex (Figure 1A). Using tryptophan fluorescence as previously described (*11*), we determined the dissociation constants of the ED-10 a-DNAb for the sequences shown in Figure 1A (Table 1).

Although the site 35 with the highest affinity is the 18mer, for 12−23 bp duplexes, the affinity remains fairly high, with a maximum difference of 0.5 kcal/mol ($2K_D$). The affinity decreases and appears to reach a plateau at 20-fold for the 48mer, and surprisingly increases again for the 80mer, with a value similar to that of the 18mer (Figure 1B and Table 1). A 166 bp fragment containing the site 35 sequence exhibits a lower affinity, following the overall trend observed with length increases (Figure 1B). The $K_D$ of the longer DNAs approaches a value between 15 and 20 nM, something substantially lower than that of the reference duplex, but still a relatively high affinity. There is a correlation between affinity and fluorescence change, with high-affinity DNA binding being accompanied by a maximum fluorescence change (Figure 1C). This is also true for the 80mer, which showed an unexpectedly high affinity. Titrations at 10, 20, and 30 nM ED-10 with the site 35-80 duplex indicate a 1:1 stoichiometry (not shown), strongly suggesting the presence of a single specific binding event.

The shortest oligonucleotide that was tested was the 10mer, since smaller duplexes would be too unstable at room temperature. This duplex displays a 10-fold lower affinity for the a-DNAb than the 18mer, an otherwise rather high affinity if we consider its absolute value of 10 nM. A single-stranded oligonucleotide forming a hairpin with a stem that mimics the 18mer duplex was found to have a 20-fold lower affinity for the a-DNAb, which is an outlier in the plot of $K_D$ versus length [Figure 1B (□)].

The a-DNAbs can discriminate a single A to T replacement at the central flexible region, corresponding to a "noncontact" region in the complex with the natural partner, the E2C domain (*12*). We analyzed another of the natural E2 sites in the upstream regulatory region of the HPV-16 genome, site 50, in which a T·A pair of the site 35 sequence changes to a C·G pair (Figure 1A). The affinity decreases 14-fold (Table 1), more drastic than the A to T replacement in the other natural E2 site, 7450, which exhibited a 3-fold decrease. Even more dramatic is the change in affinity for a bovine virus (BPV-1)-derived E2 site (*13*) with two A·T pairs at the spacer sequence being exchanged with C·G pairs (Figure 1A), reaching a 100-fold increase in $K_D$ (Table 1). However, an A10G mismatch in strand A leaves the affinity of site 35-18 intact (Table 1), suggesting that this base is not paired in the bound form, and that the base moiety does not make a direct contact with the antibody.

*The a-DNAbs Produce Partial Melting of the DNA Duplex upon Binding.* Protein secondary structure dominates the circular dichroism (CD) spectrum below 250 nm, and therefore, the region from 250 to 320 nm is preferred for the study of nucleic acid conformations bound to proteins (*14*). Figure 2A shows the near-UV CD spectrum of the site 35 double-stranded DNA oligonucleotide, with a typical composite positive band at ∼280 nm. When bound to the E2C domain, the DNA displays a blue shift in the wavelength maximum, probably due to the increase in the magnitude of the 270 nm component, and an increase in the intensity. However, the crossover band at 260 nm, corresponding to the absorption maximum, is coincident with the unbound DNA, suggesting significant but limited changes in the typical B conformation (*12*, *13*).

In the antibody-bound site 35 DNA, the blue shift is more pronounced as evidenced by a distinctive band around 270 nm and shifts in the crossover band of 1 and 3 nm for ED-10 a-DNAb and ED-84 a-DNAb, respectively (Figure 2A). The near-UV CD spectrum of heat-denatured site 35 DNA resembles that of a-DNAb-bound DNA, suggesting that substantial base unstacking is taking place.

Overall, the a-DNAbs inflict a conformational change on site 35 DNA qualitatively different from that resulting from E2C binding. Analysis of the difference spectra (Figure 2B) shows that the spectrum of the antibody-bound DNA is qualitatively similar to the spectra of the DNA at 85 °C or

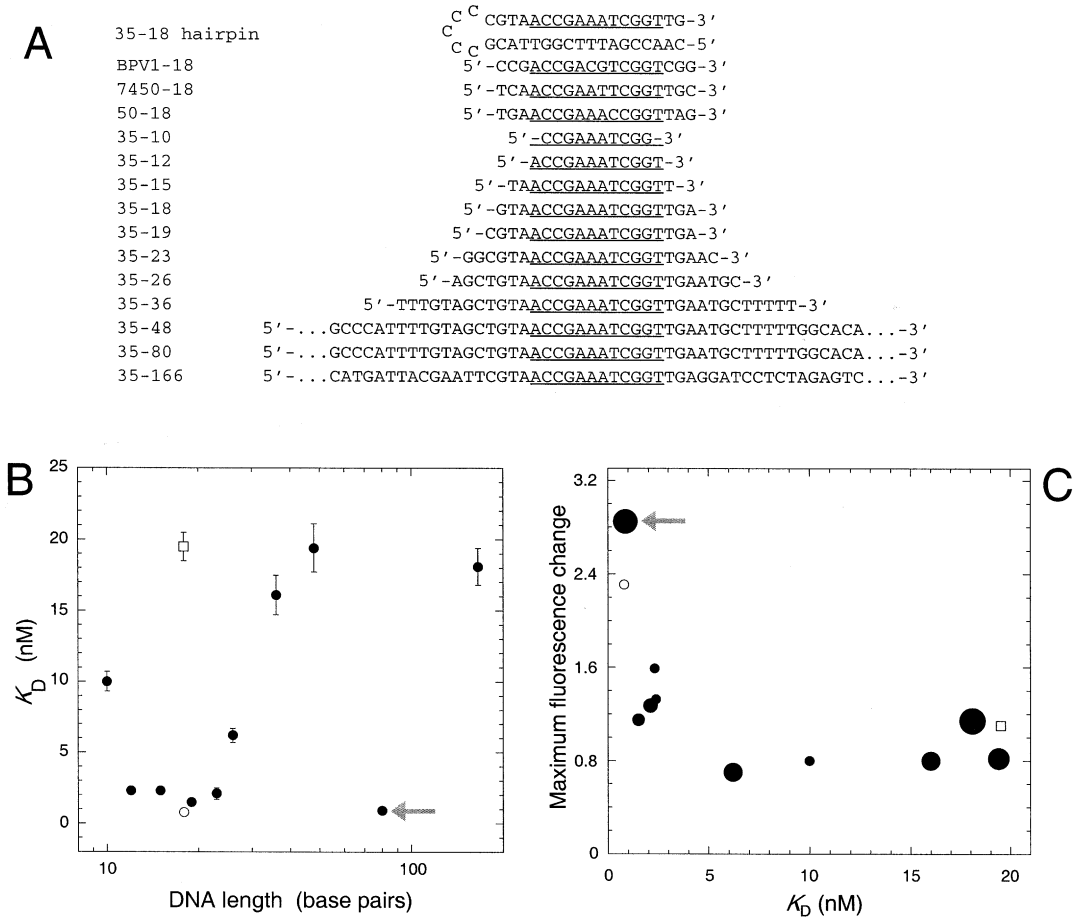


FIGURE 1: Sequence specific binding of ED-10 a-DNAb to E2 site duplexes. (A) The A chain DNA sequence of a family of oligonucleotide duplexes of increasing length (10−166 bp) that contains reference site 35 (see Materials and Methods). The 18mer sequence corresponding to site 50 and site 7450 from the HPV-16 genome and that of a bovine papillomavirus (BPV-1) are denoted as 50-18, 7450-18, and BPV1-18, respectively. A single-stranded oligonucleotide forming a hairpin with a stem that mimics the 35-18 duplex was also tested (35-18 hairpin). The underlined sequence is the consensus E2 binding site. (B) Relationship between oligonucleotide length and ED-10 a-DNAb binding affinity. Site 35-10 to site 35-166 duplexes are denoted with circles: site 35-18 (○) and site 35 in the context of oligonucleotides of different lengths (●). The site 35-18 hairpin is denoted with an empty square. The arrow points to site 35-80, showing an unexpectedly high affinity. (C) ED-10 a-DNAb fluorescence change produced by each oligonucleotide at binding saturation. Symbols are the same as in panel B. The increasing size of the circles indicates increasing oligonucleotide length from 10 to 166 bp. The arrow denotes site 35-80, with high affinity and a large fluorescence change.

in 65% methanol (not shown), where the latter is known to dehydrate B-DNA (*14*).

Melting of DNA in solution is accompanied by an increase in UV absorption at 260 nm. The decrease in absorption upon duplex formation, known as hypochromicity, is a simple and effective way to measure changes in DNA structure. Titration of a fixed concentration of the site 35 18mer duplex with ED-10 Fab shows a maximum change in $A_{260}$ of $(2.3 \pm 0.2) \times 10^{-3}$ unit, saturating at a 1:1 ratio, in agreement with fluorescence titrations (*11*) (Figure 3A). A similar titration with the E2C domain shows only a small UV absorbance change (Figure 3A).

Thermal denaturation of site 35-18 shows a cooperative transition with a total $A_{260}$ change of $(6.0 \pm 0.1) \times 10^{-3}$ unit at 25 °C (Figure 3B). This means that, upon binding, the a-DNAb causes a change in UV absorption of the DNA, and therefore base unstacking, corresponding to 40% of the change caused by thermal denaturation. An evident premelting, noncooperative transition is observed upon denaturation of site 35-18, which we ascribe to local melting of the central AAAT sequence (*15*). The total absorbance change produced upon titration becomes proportionally smaller with the increase in duplex length (Table 1).

*DNA Binding and Duplex Stability.* We analyzed the stability of the oligonucleotide duplexes of different lengths (Figure 1A) and tested for binding affinity, and the corresponding $T_m$s are shown in Table 1. The affinity becomes lower as the stability of the DNA duplexes increases, similar to what was found for DNA length (Figure 1B), with the optimal affinity around the stability and length corresponding to the site 35 18mer (Figure 3C). The site 35 hairpin, with a stem corresponding to the 18mer sequence, shows an expectedly high thermal stability, and fits in the overall correlation between affinity and stability. The 80mer that showed an affinity identical to that of site 35-18 exhibits a decrease in stability with respect to the 48mer, by a 12 °C difference in the $T_m$ (Table 1). This somehow unexpected result suggests the requirement of lower stability, in particular in the central and flexible region of the E2 site, and uncovers a link between DNA stability and binding affinity. However, the lower stability of the shorter 10- and 12mers is not translated into higher affinity, stressing the contribution of

Table 1: DNA Binding of Different E2 Site Duplexes to ED-10 a-DNAb

| DNA | $K_D$[a] (nM) | $T_m$ (°C) | ΔAbs at 260 nm[a] (% of total melting) |
|---|---|---|---|
| 35-18 hairpin | 19.5 ± 1.0 | >95 | ND[e] |
| BPV1-18 | 112 ± 5.0 | *b* | ND[e] |
| 7450-18 | 2.1 ± 1.1[c] | ND[e] | ND[e] |
| 50-18 | 14.0 ± 1.8 | 57 | ND[e] |
| 35-10 | 10.0 ± 0.7 | 29 | 65 |
| 35-12 | 2.3 ± 0.3 | 38 | 50 |
| 35-15 | 2.3 ± 0.1 | 45 | 43 |
| 35-18 | 0.8 ± 0.1 | 55 | 39 |
| 35-19 | 1.5 ± 0.2 | 57 | 29 |
| 35-23 | 2.1 ± 0.4 | 65 | 22 |
| 35-26 | 6.2 ± 0.5 | 69 | 22 |
| 35-36 | 16.1 ± 1.4 | 70 | 18 |
| 35-48 | 19.4 ± 1.7 | 75 | 15 |
| 35-80 | 0.9 ± 0.1 | 63 | ND[e] |
| 35-166 | 18.1 ± 1.3 | 86 | ND[e] |
| 35-18-A10G/A[d] | 1.8 ± 0.2 | ND[e] | ND[e] |

[a] The stoichiometry is 1:1 for all sequences that were tested. [b] This DNA displayed a complex transition. [c] Data from ref *11*. [d] The 35-18 duplex with a mismatch (A10G) in the spacer region of strand A: GTA ACC GAA GTC GGT TGA. [e] Not determined.

sequence recognition in addition to low duplex stability. The 166 bp fragment follows the overall trend of stability, affinity, and length, only interrupted by the 80mer duplex. It remains to be established how new sequence information added from the 48mer to the 80mer is capable of generating long-range interactions leading to lower stability in the E2 site, and how these revert in a longer fragment.

*DNA Binding by a-DNAbs Is Insensitive to Salt Effects.* Most protein−DNA equilibria are sensitive to changes in salt concentration; typically, their affinities decrease as the salt concentration is increased, since electrostatic interactions contribute largely to the overall stability of protein−DNA complexes (*16*). The logarithmic plot of $K_D$ versus salt concentration for the ED-10−DNA interactions shows a negligible slope, indicating insensitivity to salt effects (Figure 4A). Since changes in tryptophan fluorescence might be hampered by high ionic strength, we used an alternative method to confirm this unexpected behavior. We carried out binding experiments in solution in which the DNA-bound species (E2C, ED-10 a-DNAb, or ED-84 a-DNAb) were detected via an ELISA-based method using biotinylated DNA and streptavidin (Figure 4B). Both a-DNAbs remained bound at the highest salt concentrations that were tested. In contrast, sodium chloride concentrations of 0.5 M were enough to dissociate the E2C domain completely from the DNA, in excellent agreement with fluorescence polarization experiments in solution (Figure 4B, inset).

*Thermodynamic Characterization of DNA Binding.* Isothermal titration calorimetry (ITC) provides a direct measurement of thermodynamic parameters associated with protein−DNA interactions (*17*, *18*), allowing a comparative dissection of the DNA binding mechanism of the a-DNAbs and E2C domain. The steep change in the exothermic peak areas confirms a very tight DNA binding by the a-DNAbs (Figure 5) as well as the E2C domain (not shown). The DNA binding enthalpy for E2C is 5 kcal/mol more exothermic than those for ED-10 a-DNAb and ED-84 a-DNAb (Table 2). While the E2C−DNA interaction makes favorable enthalpic and unfavorable entropic contributions to the free energy, both antibodies show a less favorable enthalpic component

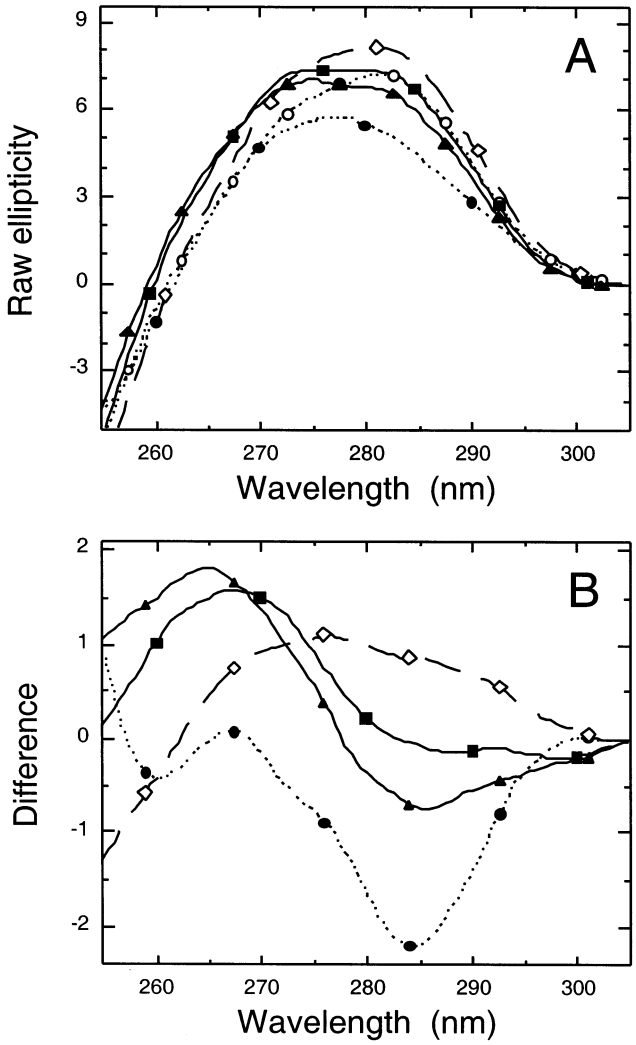


FIGURE 2: Analysis of free and bound DNA conformations by near-UV circular dichroism. Site 35-18 DNA was incubated at 2 μM in 25 mM Tris, 150 mM NaCl, and 0.1 mM DTT (pH 7.4) at 25 (○) and at 85 °C (●), or complexed with equimolar concentrations of E2C (◇), ED-10 (■), or ED-84 (▲). In the wavelength window that was used (255−305 nm), the contribution from amino acid aromatic residues is low compared to that of the DNA bases, and was subtracted (*39*). (A) Near-UV CD spectra. (B) Difference spectra, with the site 35-18 DNA spectrum subtracted.

but a more favorable entropic component (Table 2). There appears to be a compensating entropic−enthalpic effect, which results in binding free energies within the same range.

Since the protein concentrations and the binding affinities were high in the temperature range of 290−305 K, only the binding enthalpies were determined in this range. The ITC results are shown in Figure 6, in which plots of the binding enthalpies for each titration as a function of temperature are shown. The binding enthalpy of E2C−DNA interaction is temperature-dependent with a negative heat capacity change ($\Delta C_p$) as expected for typical highly complementary and specific protein−DNA interactions (*19*, *20*) (Table 2); however, both a-DNAbs display positive $\Delta C_p$ values (Figure 6). There are several sources of heat capacity changes in biochemical processes (*21*), and it is generally accepted that the major contribution comes from changes in the level of exposure of the binding surface area to solvent (*17*, *22*) from either folding, binding, or processes where local folding is coupled to binding (*20*). Several groups have developed

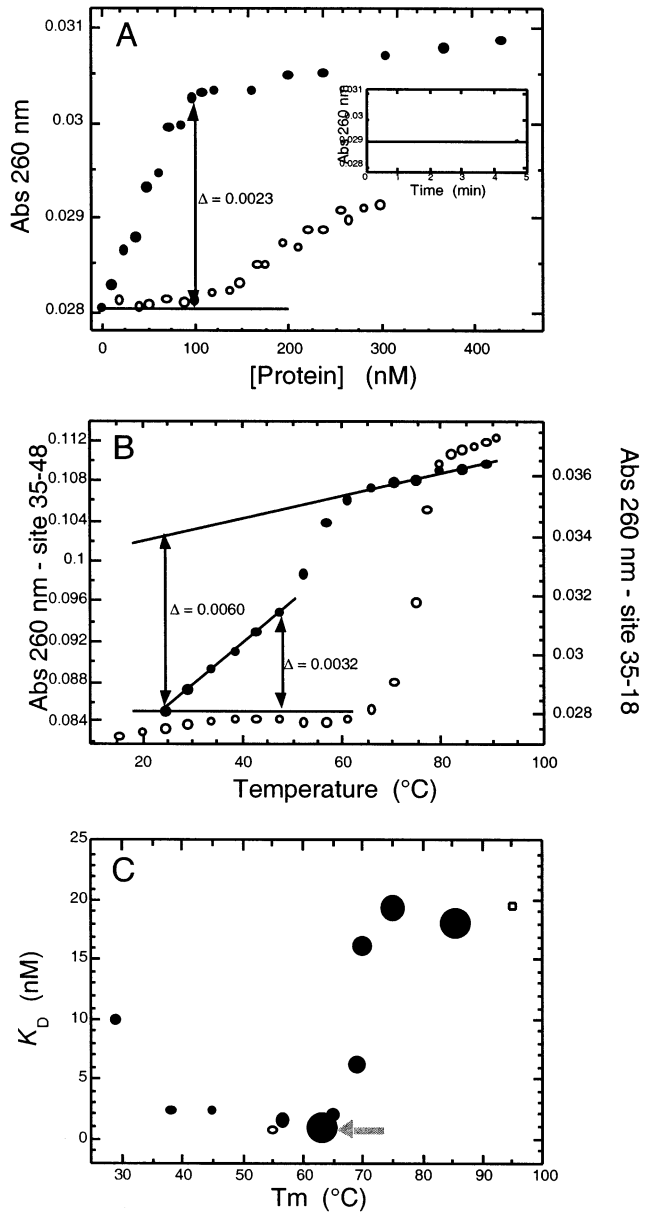


FIGURE 3: Changes in DNA conformation from UV spectroscopy: DNA denaturation and correlation between duplex stability and binding affinity. (A) Site 35-18 (100 nM) absorbance change produced by ED-10 a-DNAb (●) or E2C (○) binding. The inset shows the signal-to-noise ratio for the $A_{260}$ measurements. (B) Melting curves for site 35-18 (●) and site 35-48 (○) at 100 nM. (C) Relationship between ED-10 a-DNAb binding affinity and oligonucleotide stability ($T_m$). Symbols are the same as in Figure 1C.

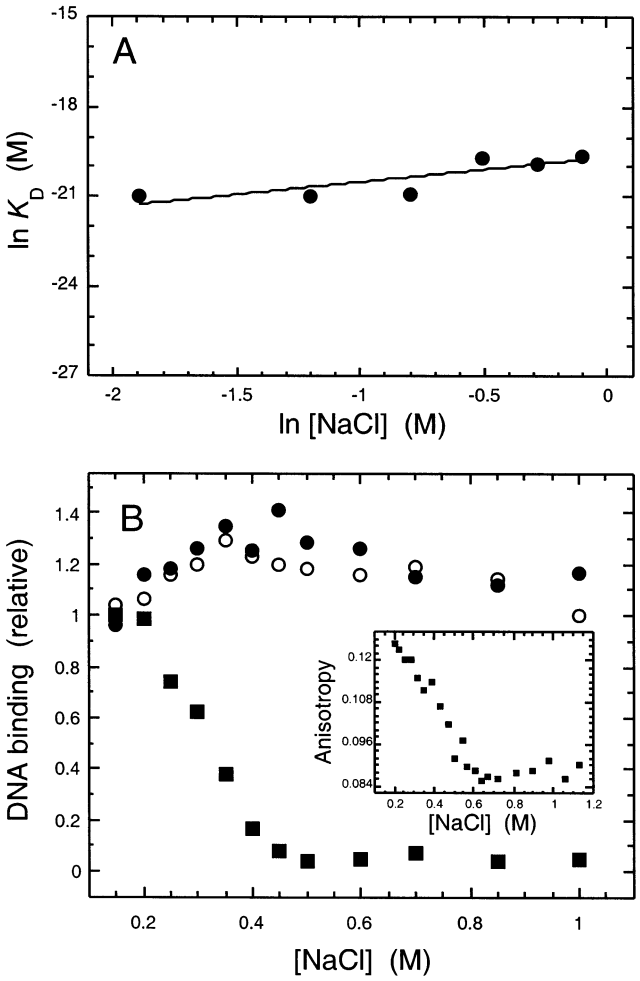


FIGURE 4: a-DNAb−DNA interaction is insensitive to salt effects. (A) Dependence of ED-10 a-DNAb affinity for site 35-18 on buffer NaCl concentrations, measured by Trp fluorescence changes. The protein concentration was 10 nM. (B) Effect of NaCl on DNA binding by E2C and a-DNAbs determined from an ELISA experiment. Details are explained in Materials and Methods: E2C (■), ED-10 (○), and ED-84 (●). The inset shows the effect of NaCl concentration on fluorescence anisotropy of fluorescein-modified site 35-18 in complex with equimolar amounts of E2C.

algorithms which assign an average contribution from apolar surface area to $\Delta C_p$ of approximately 0.4 cal mol$^{-1}$ K$^{-1}$ Å$^{-2}$. According to this, the E2C−DNA complex would bury 2600 Å$^2$, in fairly good agreement with the value of 3300 Å$^2$ calculated from the structure of the homologous BPV domain (*13*). Using the same algorithm, the a-DNAbs−DNA complexes would be exposing, rather than burying, 1100 Å$^2$ of apolar surface area. In agreement with spectroscopic results, the antibody-bound DNA could distort the DNA in such a way that base aromatic rings are exposed to the solvent, or unlikely large local folding events at the antibody binding site are taking place.

*a-DNAbs Bind DNA at a Much Slower Rate than the E2C Domain.* Kinetics of protein−DNA interactions are typically very fast, often diffusion-controlled processes, facilitated by electrostatic steering between the polyanionic DNA and the basic recognition interfaces in DNA binding proteins. As expected for a very basic dimeric DNA binding protein, E2C binds extremely fast to the 18mer site 35 duplex, with a $k_{on}$ of $1.5 \times 10^9$ M$^{-1}$ s$^{-1}$, and ED-10 a-DNAb binds 4 orders of magnitude more slowly to the same duplex (Figure 7). Although the kinetic binding mechanisms are likely to be more complex, at 0.1 $\mu$M, the half-life for a-DNAb binding to DNA is 10 s, versus a value of 0.007 s for the viral DNA binding domain.

## DISCUSSION

We have obtained anti-double-stranded DNA monoclonal antibodies against the DNA binding site of the transcriptional regulator E2 from human papillomavirus (HPV-16), and these were shown to discriminate specific double-stranded DNAs from nonspecific double-stranded DNAs and single-stranded DNAs with factors ranging from 125- to 20000-fold (*11*). Anti-double-stranded DNA autoantibodies exhib-

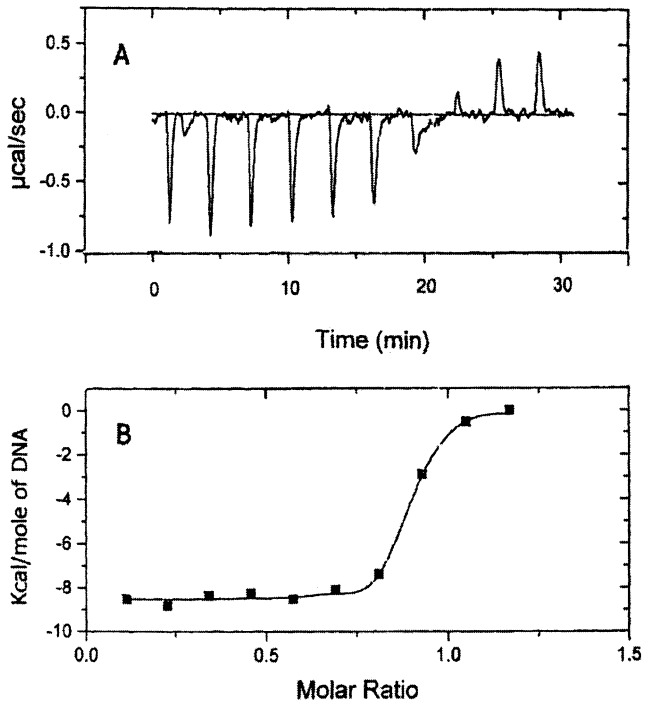


FIGURE 5: Isothermal titration calorimetry of E2C and a-DNAbs binding to DNA. (A) Titration of ED-10 a-DNAb with site 35-18. Aliquots (10 $\mu$L) of a 0.39 mM DNA solution were gradually injected into 0.024 mM ED-10 at 314 K. Similar procedures were carried out for ED-84 Fab and E2C. (B) Binding isotherm for the titration shown in panel A with the heats of DNA dilution subtracted from the observed heats. The line is from a fit of a simple 1:1 binding model to the results. This fit yielded a stoichiometry of $0.84 \pm 0.01$, a binding enthalpy of $-8.5 \pm 0.1$ kcal/mol, and a $K_D$ of $33 \pm 2$ nM ($\Delta G = -10.8 \pm 0.2$ kcal/mol). The calculated binding enthalpies are displayed in Table 2.

Table 2: Thermodynamic DNA Binding Parameters

| protein | temp (K) | $\Delta G$ (kcal/mol) | $\Delta H$ (kcal/mol) | $T\Delta S$ (kcal/mol) | $\Delta C_p$ (cal mol$^{-1}$ K$^{-1}$) |
|---|---|---|---|---|---|
| E2C | 302.5 | −13.1 | $-15.2 \pm 0.8$ | $-2.1 \pm 0.8$ | $-338 \pm 38$ |
| E2C[a] | 301.8 | − | $-15.2 \pm 0.8$ | − | $-370 \pm 50$ |
| ED10 | 303.1 | −12.4 | $-10.0 \pm 0.1$ | $2.4 \pm 0.1$ | $95 \pm 16$ |
| ED84 | 301.2 | −11.7 | $-10.4 \pm 0.1$ | $1.3 \pm 0.1$ | $90 \pm 29$ |

[a] Inverse titration, i.e., gradual addition of E2C protein to DNA.

ited low affinities, and little discrimination capacity (*7*, *8*). Moreover, it is not yet clear which antigenic sequence elicited them. Although there is no direct link to autoimmune pathogenesis, the a-DNAbs presented here are the first example of a specific and high-affinity response to a predetermined double-stranded DNA target. The recognition mechanism is radically different from that of natural DNA binding proteins and appears to have no similarities with that of the pathogenic a-DNA autoantibodies.

ED-10 a-DNAb is able to recognize a sequence of the E2 site 35 duplex with as few as 10 bp, with a $K_D$ of 10 nM, a still rather high affinity compared with those of nonspecific duplexes (Figure 8). The highest affinity that is displayed is toward the reference antigenic sequence, where we consider optimal length recognition an additional indicator of the specificity of the a-DNAb. The affinity is therefore optimized for the 18mer sequence, but it binds with overall high affinity to the DNAs of different lengths that include the E2 site 35 sequence (Figure 8). These a-DNAbs clearly have the

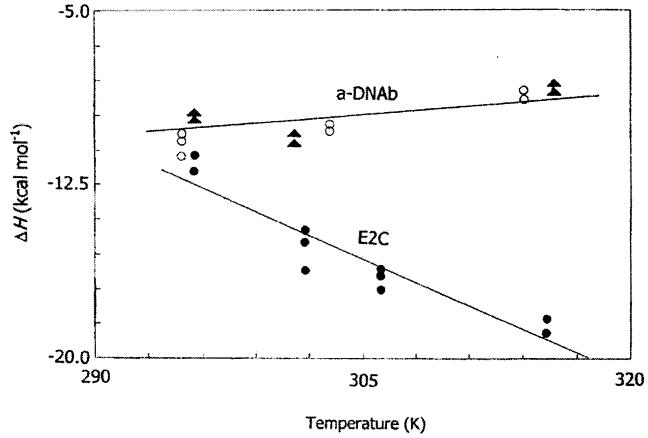


FIGURE 6: Binding enthalpies as a function of temperature for ED10 a-DNAb (○), ED84 a-DNAb (▲), and E2C (●). Since the temperature dependencies of the a-DNAb binding enthalpies were close, they were fitted to the same straight line. The slopes of the fits are presented in Table 2.

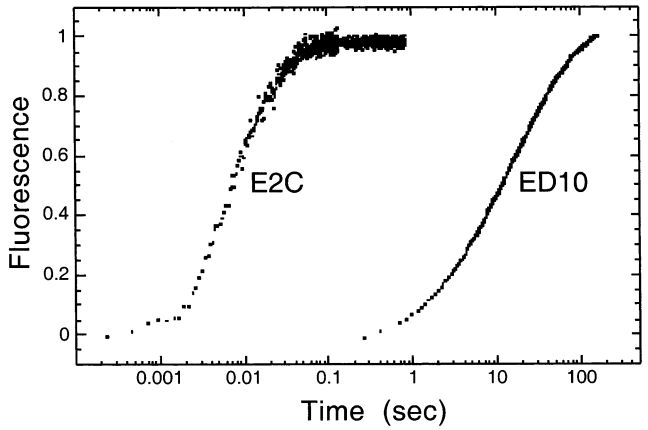


FIGURE 7: DNA binding rates of E2C and ED-10. Kinetic DNA binding experiments were carried out using SX 18MV stopped-flow equipment from Applied Photophysics. E2C at 200 nM was mixed with fluoresceinated site 35 DNA (*40*) in equimolar concentrations, and fluorescein fluorescence was followed. For ED-10 a-DNAb, a 1:1 mixture of 200 nM antibody and unmodified site 35 DNA duplex was mixed, and the tryptophan fluorescence change was followed. In both cases, the data were fitted to a second-order equation with an exponential term (*41*) with $k_{on}$ values of $1.5 \times 10^{-9}$ and $1.0 \times 10^{-5}$ M$^{-1}$ s$^{-1}$ for E2C and ED-10 DNA binding, respectively.

potential to recognize the site 35 DNA sequence in the context of larger genomic fragments.

The a-DNAbs are capable of discrimination of single-base changes present in the central region, defined as flexible (*12*). Among the two natural HPV-16 E2 sites, the antibody exhibits a lower affinity for site 50, which includes a C·G pair instead of a T·A pair (see Figure 1A). A bovine virus-derived sequence, used in crystallographic studies of the BPV1−DNA complex (*13*), bears an ACGT sequence instead of an AAAT sequence in the central region, and its affinity approaches nonspecific binding (Figure 8).

A link between stability and affinity for the specific DNAs is clear for the hairpin single-stranded oligonucleotide with a stem that mimics the 18mer site 35 reference duplex. Although the sequence presented for binding is equivalent to an 18mer double-stranded DNA, the $T_m$ of the hairpin is at least 40 °C higher and the $K_D$ changes to 20 nM. The 48mer duplex displays a similar affinity value and a $T_m$ of

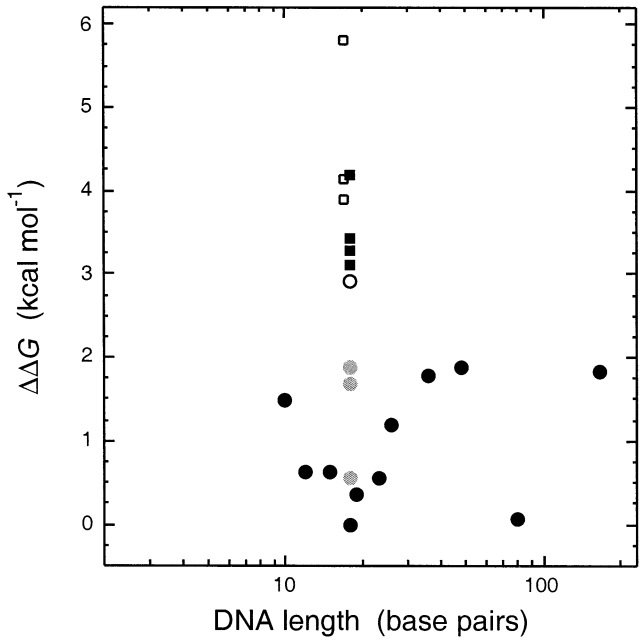


FIGURE 8: Difference in the free energy of binding of ED-10 a-DNAb to different DNA duplexes. The $K_D$s from Table 1 were converted into $\Delta G$ values ($\Delta G = -RT \ln K$), and the energy difference between each duplex and reference site 35 ($\Delta\Delta G$) was plotted vs DNA duplex length on a logarithmic scale: (●) site 35-10 to site 35-166 duplexes (see Table 1), (gray circles) from top to bottom, 35-18 hairpin, 50-18, and 7450-18 duplexes, (○) BPV1-18 site, (■) from top to bottom, EBNA, HPV-16-2300, CRE, and ARC 18mer duplexes, (□) single-stranded DNAs, from top to bottom, site 35-A, ARC, and HPV-16-2300.

75 °C. The high affinity for the 80mer duplex is quite surprising, as is the lower stability of this duplex to thermal denaturation, with a $T_m$ that is 12 °C lower than that of the shorter 48mer. In addition, the tryptophan fluorescence change in the a-DNAb upon binding of the 80mer is maximal, correlating with tight binding (Figure 1C). In any case, both the HPV-16 site 50 and BPV1-derived 18mer duplexes exhibit different affinities despite the similar length. We propose that the lower stability of the DNA cooperates with sequence recognition in producing the highest binding affinity. Although the hypochromicity caused by Fab binding to the DNA would suggest five to seven melted base pairs, we do not have enough information to ascertain a behavior identical to that of a full thermal melting of the DNA. The alteration in the DNA structure appears to be independent of the length, but the local stability of the unstacked region will be influenced by the number and sequence of flanking base pairs.

Loss of hydrogen bonding and hydrophobic interactions in DNA results in conformational changes which may ultimately lead to dehydration and unstacking. Water plays a key role in DNA stabilization in solution, and both the removal of ordered waters and the exposure of aromatic hydrophobic base rings must impose a distortion on the DNA, in agreement with the circular dichroism results, showing a resemblance between a-DNAb-bound DNA and thermally denatured or methanol-dehydrated DNA. In addition, while E2C causes a minimal change in UV absorption at 260 nm upon binding to DNA, in agreement with structures of E2−DNA complexes (*12*, *13*, *23*), ED-10 a-DNAb causes an hyperchromicity in the 18mer site 35 DNA duplex corresponding to 40% of the absorbance change produced by full thermal denaturation. A noncooperative premelting transition in the thermal denaturation curve indicates local DNA melting most likely in the central AAAT sequence of site 35-18 (*15*). Therefore, combining CD and UV absorption results, we have shown that the DNA undergoes a large structural change upon binding to the a-DNAbs, involving extensive base unstacking.

A reduction in the DNA binding affinity with increased salt concentrations is typical of sequence specific DNA binding and is related to counterion release from DNA (*24*). A unique exception is the binding of the TATA box binding protein (binds DNA at high salt concentrations) from the hyperthermophilic archaeon *Pyrococcus woesei*, which lives in highly saline conditions (*25*). The a-DNAbs bind DNA tightly at up to 1.2 M salt, in clear contrast with the E2C domain. The effect of salts on a particular equilibrium is the result of polyelectrolyte, Hofmeister, and osmotic effects (*26*). Despite these individual contributions not being clearly separable at this stage, electrostatic interactions do not play a significant role in the a-DNAb−DNA interaction, the opposite of what is usually observed for natural DNA binding proteins. Inspection of the CDR regions in H and L chains of both antibodies does not reveal the presence of an excess of positively charged residues as proposed for autoimmune a-DNA antibodies (*27*, *28*) and normally found in natural DNA binding domains (*3*). Strong Coulombic interactions between a-DNAbs and the DNA polyanion are clearly not involved.

Salt concentrations in the molar range are also expected to reduce the thermodynamic activity of water (*26*). The insensitivity of the a-DNAb−DNA interaction to solute effects suggests that there are fewer water molecules involved in this interaction than in the E2−DNA interface [there are 28 water molecules present in the BPV E2−DNA complex (*13*)] and that any water molecules that remain must be strongly bound. On the basis of the insensitivity to salt effects, we rule out cation release from the DNA polyanion as the source of positive entropic change. Our hypothesis is that the main component in the favorable entropic contribution is the hydrophobic effect, i.e., the release of ordered waters from the hydrophobic surface of both antibodies and DNA. However, we need to accumulate more evidence to prove this hypothesis. The HCDR3 of both antibodies bears four aromatics out of nine residues, which supports this hypothesis (*11*). Such a possibility requires a strong interaction of the a-DNAb binding site side chains with the DNA base aromatic rings, and must involve a substantial conformational change. This agrees with our CD and UV absorption results indicating structural changes in DNA, and with the correlation between high affinity and local melting in the central A/T rich region. This "opening" of the DNA duplexes favoring recognition would suggest that the antibodies could at least in part recognize single-stranded DNA. However, the high-stability duplexes that were tested, and in particular those with ≥18 bp, are unlikely to be dissociated into single strands. This is also true for the hairpin with a stem that mimics the 18mer duplex.

Single-stranded DNA oligonucleotide ligands were selected from random libraries as high-affinity binders for lupus autoantibodies (*29*). One of these antibodies, 11F8, was shown to discriminate a particular selected sequence from

other single-stranded ligands (*9*). ssDNA binding by this antibody was largely enthalpically driven, with an unfavorable entropy term, contrary to the anti-double-stranded DNA antibodies we now describe. In addition, they exhibited a negative heat capacity change as seen in natural protein−DNA interactions, but not in the a-DNAbs we describe (*10*). We propose that the structural change in the DNA with substantial base unstacking, in combination with local strand separation of the specific site 35 DNA duplex, leads to an increase in exposed surface area, providing an explanation of the unusual positive $\Delta C_p$. However, other as yet unknown sources of $\Delta C_p$, in addition to surface area, must be contributing to this particular phenomenon (*21*, *30*).

A detailed thermodynamic analysis of DNA melting revealed that this process is accompanied by a positive $\Delta C_p$, with an average value of 64 cal $mol^{-1}$ $K^{-1}$ per base pair for mainly polyd(AT)·polyd(AT) duplexes (*31*). The antibody-bound DNA displays an average value of 9.1 cal $mol^{-1}$ $K^{-1}$ per base pair, so if one assumes a burial of amino acid residues on the antibody surface that will contribute negatively [with a conservative average estimate of 10.0 cal $mol^{-1}$ $K^{-1}$ or 52 $Å^2$ per residue (*32*)], there must be significant deviation from the duplex B conformation in the bound DNA, the structural basis of which remains to be determined.

The association rate for the a-DNAb−DNA interaction is 4 orders of magnitude lower than that of the E2−DNA complex, which is above the limit for a diffusion-controlled reaction typical of an electrostatically favored collision. In agreement with the equilibrium spectroscopic and thermodynamic results, the slower on-rate for the a-DNAb−DNA interaction suggests a substantial rearrangement in the DNA, increasing the energy barrier to overcoming the transition state. However, antibody interactions with protein antigens are usually not much faster than $10^5$−$10^6$ $M^{-1}$ $s^{-1}$ (*33*). One can speculate that antibodies do not require faster on-rates for the *in vivo* interaction with macromolecules, and therefore, kinetic maturation beyond those limits is not necessary. In addition, a-DNAbs do not make use of electrostatic interactions as a main source for the stabilization of ground and transition states for DNA recognition. A detailed examination of the kinetic mechanism will allow us to dissect the precise order of events of a-DNAb−DNA binding.

A recent thorough investigation of the kinetic binding mechanism of the 11F8 autoantibody and its selected single-stranded DNA ligand showed a slightly faster association rate for the reference 11F8-WtDNA sequence ($10^6$ $M^{-1}$ $s^{-1}$) with respect to the a-DNAbs, proposed to be driven by electrostatic steering (*10*). Therefore, although there are a few common features between the a-DNAbs and the anti-single-stranded DNA autoantibodies, their recognition mechanisms differ substantially.

While there are more than 500 protein−DNA structures, there are only two structures of antibodies bound to DNA, the 2.7 Å BV04-01−dT3 (*42*) and the 2.1 Å DNA-1−dT6 (*43*) complexes. The latter recognizes primarily the DNA bases, while the former recognizes the backbone. Despite the low affinity of the ligand, the DNA-1−dT6 complex provides relevant details about how the recognition of DNA bases takes place. The thymine bases are stacked between tyrosine residues from both heavy and light chains (*43*), whereas BV04-01 uses a tryptophan-tyrosine pair to stack between thymine bases (*42*). The unstacking of bases in the duplex DNA caused by the a-site 35 DNA antibodies could well be linked to similar aromatic side chain−base interactions. While neither sequence of the a-site 35 DNA antibodies is similar with those of the CDRs of BV04-01 and DNA-1, the participation of hydrophobic interactions with DNA bases appears to be a common theme. However, the anti-E2 DNA antibodies are completely insensitive to ionic strength, and the thermodynamic parameters are slightly different, in particular the $T\Delta S$ term.

The a-DNAbs specifically bind to the E2 site 35 DNA sequence within duplexes of different lengths; however, they recognize the target sequence through a strategy completely different from that of the E2 protein. The results presented here indicate that binding of site 35 DNA to its natural partner, the HPV-16 E2C domain, (i) is predominantly enthalpically driven with major contributions from hydrogen bonding, either directly or water-mediated, as well as electrostatic components, (ii) retains the native B-conformation in the DNA, (iii) shows a negative $\Delta C_p$, typical of specific protein−DNA interactions and normally ascribed to burial of surface area, (iv) displays an expected high sensitivity to salt effects, and (v) displays a very fast ($>10^9$ $M^{-1}$ $s^{-1}$) association rate, in agreement with an electrostatically assisted diffusion-controlled collision.

On the other hand, the specific a-DNAb−DNA interaction (i) has a favorable entropic component in addition to the enthalpic contribution, (ii) is insensitive to high salt effects, indicating a lack of Coulombic contribution and minimal if any water-mediated interactions, possibly with a low hydrogen bonding component, (iii) requires a substantial conformational change in the bound DNA that resembles more closely a denatured or dehydrated form than the classical B-conformation, (iv) displays an unusual positive $\Delta C_p$, suggesting a certain degree of surface exposure rather than burial, and (v) binds 4 orders of magnitude more slowly than the E2C, suggesting structural rearrangements in the form of local opening of the DNA double helix preceding or in parallel with the binding collision.

The results presented here, together with the structural information from the homologous bovine protein−DNA complex, indicate that, while the natural HPV-16 E2C domain uses a direct readout mechanism for DNA recognition (*3*, *34*), the antibody strategy appears to be a distinctive case of specific indirect readout with a severe distortion of the classical B-DNA double helix. As a consequence, the complementarity in the specific antibody−DNA interface would be mediated by hydrophobic interactions predominating over the typical hydrogen bonding and water molecule pattern in conjunction with a strong electrostatic component in naturally occurring protein−DNA interactions. Considering that the architecture of antibody binding sites did not evolve for DNA binding for gene regulation purposes, the recognition mechanism characterized here perhaps represents a strategy through which the immune system could recognize DNA tightly and specifically as an antigen. Detailed atomic structures and further thermodynamic binding analysis will shed light on this puzzling novel protein−DNA recognition interface.

## ACKNOWLEDGMENT

We thank Robyn Stanfield for helpful comments.

## REFERENCES


1. Luscombe, N. M., Laskowski, R. A., and Thornton, J. M. (2001) *Nucleic Acids Res. 29*, 2860−2874.
2. Garvie, C. W., and Wolberger, C. (2001) *Mol. Cell 8*, 937−946.
3. Blackburn, G. M., and Gait, M. J. (1996) in *Nucleic acids in chemistry and biology*, Oxford University Press, New York.
4. Braden, B. C., and Poljak, R. J. (1995) *FASEB J. 9*, 9−16.
5. Davies, D. R., and Cohen, G. H. (1996) *Proc. Natl. Acad. Sci. U.S.A. 93*, 7−12.
6. Stollar, B. D. (1986) *CRC Crit. Rev. Biochem. 20*, 1−36.
7. Stollar, B. D. (1994) *FASEB J. 8*, 337−342.
8. Stollar, B. D., Zon, G., and Pastor, R. W. (1986) *Proc. Natl. Acad. Sci. U.S.A. 83*, 4469−4473.
9. Stevens, S. Y., and Glick, G. D. (1999) *Biochemistry 38*, 560−568.
10. Ackroyd, P. C., Cleary, J., and Glick, G. D. (2001) *Biochemistry 40*, 2911−2922.
11. Cerutti, M. L., Centeno, J. M., Goldbaum, F. A., and de Prat-Gay, G. (2001) *J. Biol. Chem. 276*, 12769−12773.
12. Rozenberg, H., Rabinovich, D., Frolow, F., Hegde, R. S., and Shakked, Z. (1998) *Proc. Natl. Acad. Sci. U.S.A. 95*, 15194−15199.
13. Hegde, R. S., Grossman, S. R., Laimins, L. A., and Sigler, P. B. (1992) *Nature 359*, 505−512.
14. Johnson, W. C. J. (1996) Determination of the conformation of nucleic acids by electronic CD, in *Circular Dichroism and the conformational analysis of biomolecules* (Fasman, G. D., Ed.) Vol. 12, pp 433−468, Plenum Press, New York.
15. Xu, D., Evans, K. O., and Nordlund, T. M. (1994) *Biochemistry 33*, 9592−9599.
16. Record, M. T., Jr., Lohman, M. L., and De Haseth, P. (1976) *J. Mol. Biol. 107*, 145−158.
17. Ladbury, J. E., and Chowdhry, B. Z. (1996) *Chem. Biol. 3*, 791−801.
18. Plum, G. E., and Breslauer, K. J. (1995) *Curr. Opin. Struct. Biol. 5*, 682−690.
19. Ha, J.-H., Spolar, R. S., and Record, M. T., Jr. (1989) *J. Mol. Biol. 209*, 801−816.
20. Spolar, R. S., and Record, M. T., Jr. (1994) *Science 263*, 777−784.
21. Sturtevant, J. M. (1977) *Proc. Natl. Acad. Sci. U.S.A. 74*, 2236−2240.
22. Gomez, J., and Freire, E. (1995) *J. Mol. Biol. 252*, 337−350.
23. Hegde, R. S., and Androphy, E. J. (1998) *J. Mol. Biol. 284*, 1479−1489.
24. Record, M. T., Jr., Ha, J. H., and Fisher, M. A. (1991) *Methods Enzymol. 208*, 291−343.
25. O'Brien, R., DeDecker, B., Fleming, K. G., Sigler, P. B., and Ladbury, J. E. (1998) *J. Mol. Biol. 279*, 117−125.
26. Record, M. T., Jr., Zhang, W., and Anderson, C. F. (1998) *Adv. Protein Chem. 51*, 281−353.
27. Krishnan, M. R., Jou, N., and Marion, T. N. (1996) *J. Immunol. 157*, 2430−2439.
28. Radic, M. Z., and Weigert, M. (1994) *Annu. Rev. Immunol. 12*, 487−520.
29. Swanson, P. C., Ackroyd, C., and Glick, G. D. (1996) *Biochemistry 35*, 1624−1633.
30. Janin, J. (1997) *Structure 5*, 473−479.
31. Chalikian, T. V., Volker, J., Plum, G. E., and Breslauer, K. J. (1999) *Proc. Natl. Acad. Sci. U.S.A. 96*, 7853−7858.
32. Myers, J. K., Pace, C. N., and Scholtz, J. M. (1995) *Protein Sci. 4*, 2138−2148.
33. Foote, J., and Eisen, H. N. (1995) *Proc. Natl. Acad. Sci. U.S.A. 92*, 1254−1256.
34. Travers, A. (1993) *DNA-protein interactions*, Chapman & Hall, London.
35. Mok, Y. K., de Prat Gay, G., Butler, P. J., and Bycroft, M. (1996) *Protein Sci. 5*, 310−319.
36. Cantor, C. R., Warshaw, M. M., and Shapiro, H. (1970) *Biopolymers 9*, 1059−1077.
37. de Prat Gay, G., and Fersht, A. R. (1994) *Biochemistry 33*, 1957−1963.
38. Schwarz, F. P., Tello, D., Goldbaum, F. A., Mariuzza, R. A., and Poljak, R. J. (1995) *Eur. J. Biochem. 228*, 388−394.
39. Gray, D. M. (1996) Circular Dichroism of protein-DNA interactions, in *Circular Dichroism and the conformational analysis of biomolecules* (Fasman, G. D., Ed.) Vol. 12, Chapter 13, pp 469−500, Plenum Press, New York.
40. Ferreiro, D. U., et al. (2000) *Biochemistry 39*, 14692−14701.
41. de Prat Gay, G., Ruiz-Sanz, J., and Fersht, A. R. (1994) *Biochemistry 33*, 7964−7970.
42. Herron, J. N., et al (1991) *Proteins: Struct., Funct., Genet. 11*, 159−175.
43. Tanner, J. J., Komissarov, A. A., and Deutscher, S. L. (2001) *J. Mol. Biol. 314*, 807−822.


BI026866U